JOURNAL OF AIRCRAFT
Vol. 37, No. 1, January–February 2000

Transonic-Aerodynamic-Influence-Coefficient Approach for Aeroelastic and MDO Applications

P. C. Chen* and D. Sarhaddi†
ZONA Technology, Inc., Scottsdale, Arizona 85251
and
D. D. Liu‡
Arizona State University, Tempe, Arizona 85287

A developed transonic-aerodynamic-influence-coefficient (TAIC) method is proposed as an efficient tool for applications to flutter, aeroservoelasticity, and multidisciplinary design/analysis optimization. Several plausible procedures for AIC generation are described. The modal-based AIC procedure is formally established as a general AIC scheme applicable to all classes of computational fluid dynamics (CFD) methods. The present TAIC method integrates the previous transonic equivalent strip (TES) method with the modal AIC approach; its computer code ZTAIC has a similar input format to that of doublet lattice method (DLM) except with the additional steady pressure input. The versatility of ZTAIC is shown by two sets of cases studied: those cases with pressure input from measured data and those from CFD computation. Computed results of unsteady pressures and flutter points are presented for six wing planforms. In contrast to the usual CFD practice, the effective use of the modal AIC in ZTAIC is clearly demonstrated by the flutter calculations of the weakened and solid 445.6 wings, where the CPU time of a transonic flutter point using warm-started AIC is less than 1 min on a SUN SPARC20 workstation. Moreover, the AIC capability allows ZTAIC to be readily integrated with structural finite element method (FEM). Hence, it is most suitable to be adopted in a multidisciplinary design (MDO) environment such as ASTROS.

Introduction

RAPID progress in aeroservoelasticity and multidisciplinary design/analysis optimization (MDO/MAO) in recent years has demanded further improvement of computational aerodynamic methods in their capability to generate *s*-domain aerodynamics, their compatibility with structural finite element method (FEM), and their expediency for design optimization. The linearization of the unsteady subsonic/supersonic flow leads to the aerodynamic influence coefficient (AIC) formulation,[1–5] a procedure that is fully compatible with the structural FEM. With Roger's approximation or Karpel's Minimum-State Technique,[6,7] the *s*-domain aerodynamics can be readily generated from the *k*-domain solution yielded by the AIC approach.

In the transonic and hypersonic flow regimes the shock wave from wing (body) thickness renders the problem nonlinear and the mean flow nonuniform (for an unsteady problem). Thus, the current treatment in the unsteady transonics/hypersonics mostly adopts the computational fluid dynamics (CFD) methodology. Currently there exist a number of well-practiced CFD unsteady transonic methods[8,9] ready for aeroelastic applications. However, their acceptance by the aerospace industry for rapid analysis and design is hampered by problems in grid generation, CFD/computational structural dynamics interfacing, and affordable computing time. Their further integration into an MDO environment such as ASTROS[10,11] is somewhat discouraged by their incompatibility with the structural FEM.

Although current CFD efforts[12] are directed toward meeting the FEM compatibility, questions of affordable computing time for each MDO cycle remain outstanding. Toward this end, we have reexamined the unsteady transonic/hypersonic aerodynamic methodology critically from the viewpoint of its FEM compatibility and its expediency in an MDO environment. The result of this reexamination effort is the development of a unified AIC (UAIC) approach[13] for unsteady aerodynamics covering all Mach-number ranges. The unified supersonic/hypersonic AIC approach has been reported elsewhere.[14,15] This paper attempts to address mainly the transonic AIC approach out of this UAIC approach.

Modal-Based AIC

A formal AIC matrix should contain purely aerodynamic information relevant to the governing equation. However, to generate this type of AIC from CFD methods remains a major undertaking. On the other hand, the modal perturbation concept suggests that an expedient modal-based AIC procedure can be developed accordingly. Unlike the formal AICs, the modal-based AICs contain modal information in addition to the aerodynamics.

Consider a typical CFD computation procedure, in which the unsteady pressure is related to structural modes by

$$\Delta C_{P_{ij}} = \mathcal{N}(\phi_{ij}) \tag{1}$$

where $\mathcal{N}$ is a nonlinear CFD operator and $\phi_{ij} = \phi_i(x_j)$ are the baseline normal modes. The index i denotes the mode number and x_j the position vector. Once again, the amplitude linearization principle must be reiterated, that is, the linearization of the aerodynamics for an aeroelastic system in any flow regime can be assured if the modal amplitude is kept sufficiently small at all times. In particular, Dowell et al.[16] have established such a principle for transonic flow. With this principle imposed the operator $\mathcal{N}$ can be approximated by a linear operator $\mathcal{L}$. The pressure computation can be carried out more expediently by a linearized procedure such as the indicial method; thus,

$$\Delta C_{P_{ij}} = \mathcal{L}(\phi_{ij}) \tag{2}$$

Next, let the given structural deformation, or the given k number of modes be represented by the baseline modes, i.e.,

$$h_{kj} = \phi_{ij} q_{ki} \tag{3}$$

where q_{ki} are the best-fit coefficients to be determined by the following least-squares procedure

$$q_{ki} = \left[\left(\phi_{ij}^T \phi_{ij} \right)^{-1} \phi_{ij}^T \right] h_{kj} \tag{4}$$

Presented as Paper 97-1181 at the AIAA/ASME/ASCE/AHS/ASC 38th Structures, Structural Dynamics, and Materials Conference, Kissimmee, FL, 7–10 April 1997; received 19 June 1997; revision received 15 March 1999; accepted for publication 18 July 1999.

*Vice President; pc@zonatech.com.
†Member of Technical Staff.
‡Professor, Department of Mechanical and Aerospace Engineering. Associate Fellow AIAA.

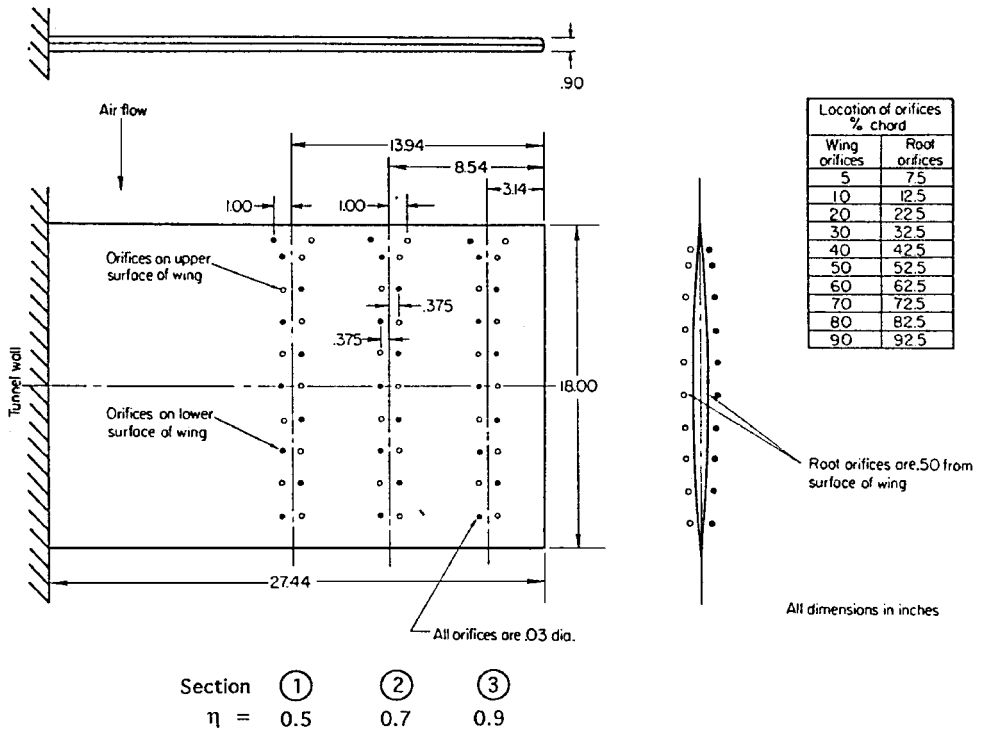

Fig. 1 Lessing wing. Configuration shows the following dimensions: AR = 3.0, 5% parabolic arc airfoil section (taken from NASA TND-344 by H. C. Lessing and J. L. Troutman).

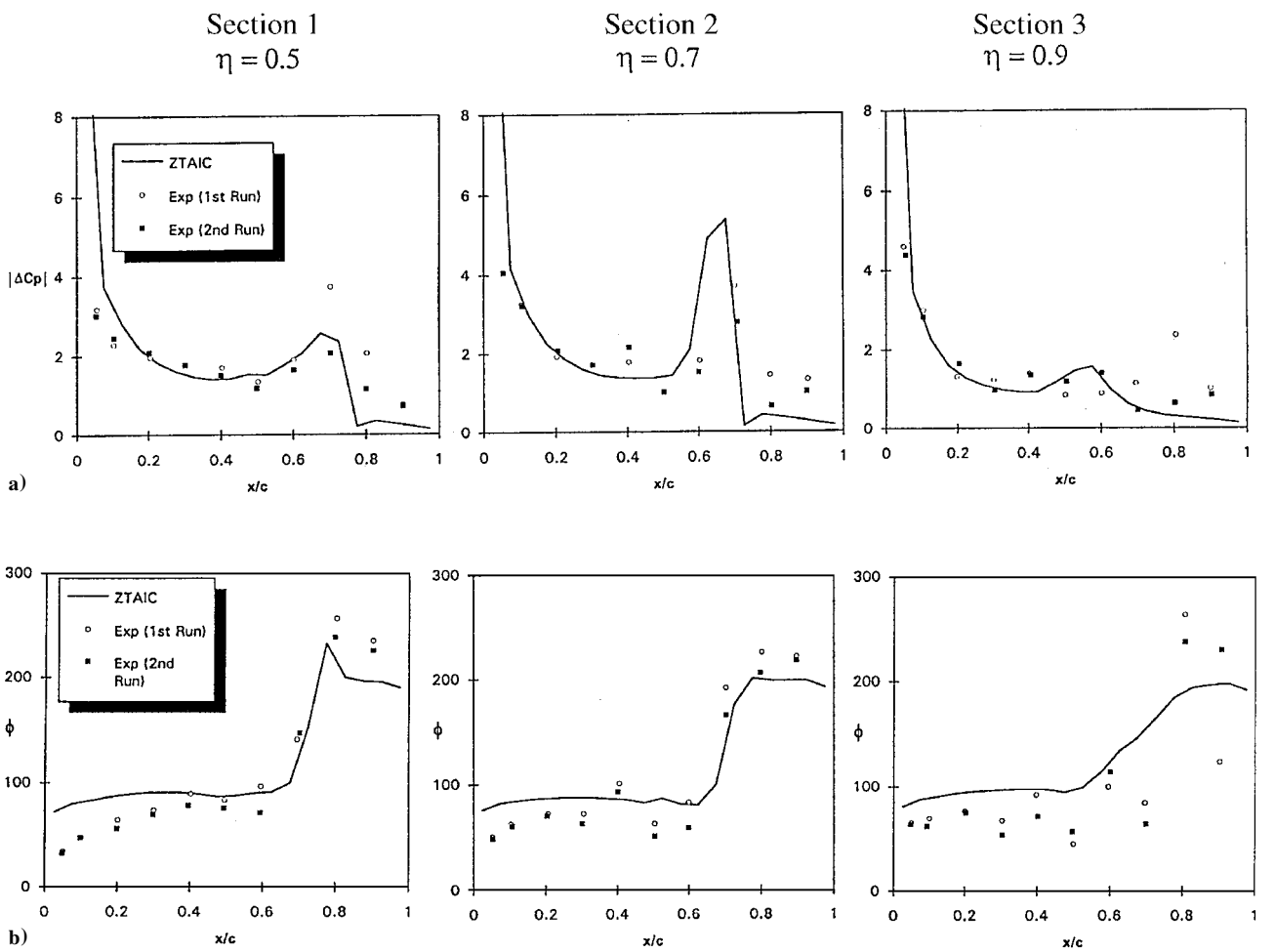

Fig. 2 Lessing wing. Unsteady pressures in terms of a) magnitude of the first bending and b) phase angle (in degrees) of the first bending (M = 0.9 and k = 0.13).

The computed pressures are related to this given set of modes by the same linear operator

$$\Delta C_{P_{kj}} = \mathcal{L}(h_{kj}) \tag{5}$$

where the linear operator reads

$$\mathcal{L}(\cdot) = \left[\Delta C_{P_{ij}} (\phi_{ij}^T \phi_{ij})^{-1} \phi_{ij}^T\right] \tag{6}$$

Symbolically, Eqs. (5) and (6) amount to

$$\{\Delta C_P\} = [A_m]\{h\} \tag{7}$$

Notice here that the ΔC_P is related to the mode shape h rather than the downwash w in a formal AIC formulation. The modal-based matrix $[A_m]$ contains intrinsically all of the necessary aerodynamic information as provided by the baseline pressure-mode relation Eq. (2). The present AIC procedure is not confined to a particular set of CFD methods. Furthermore, in a structural design loop

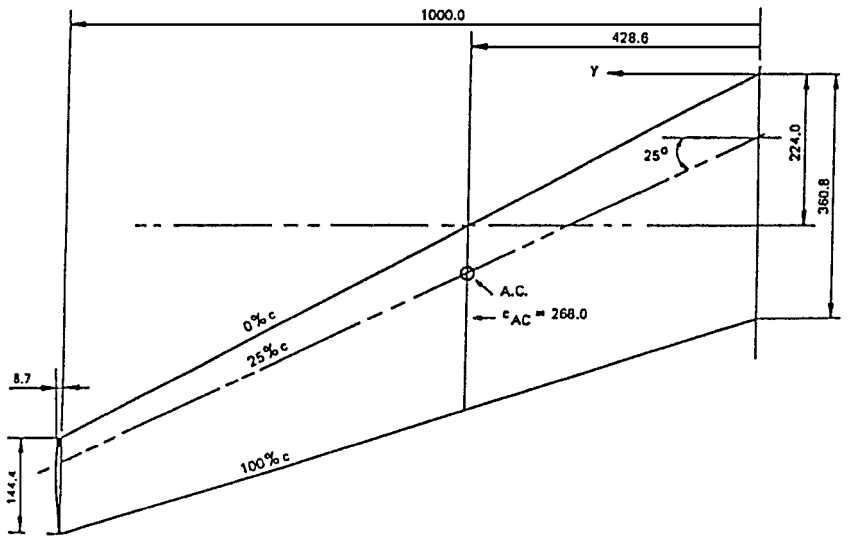

Fig. 3 LANN wing. Configuration shows the following dimensions: AR = 7.92, Λ = 25 deg, 12%-thick supercritical airfoil (taken from AFWAL-TR-83-3006 by J. B. Malone and S. Y. Ruo).

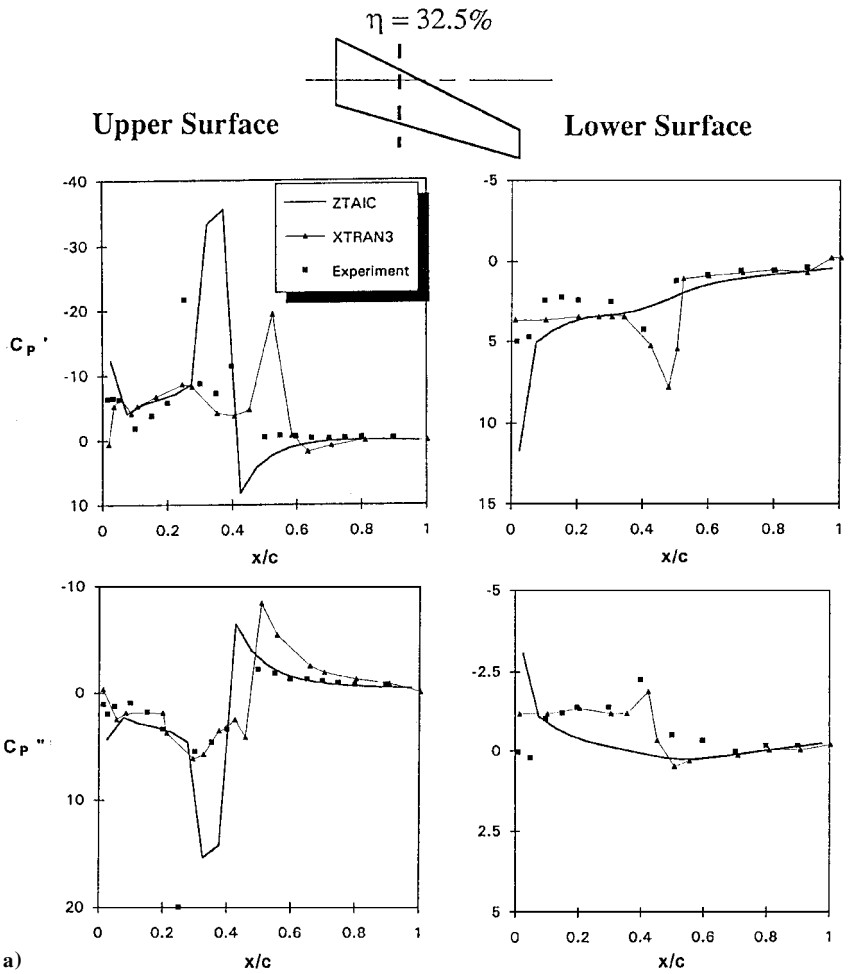

Fig. 4 LANN wing. In-phase and out-of-phase pressures in pitching oscillation about 62% root chord at three spanwise locations (M = 0.82 and k = 0.205).

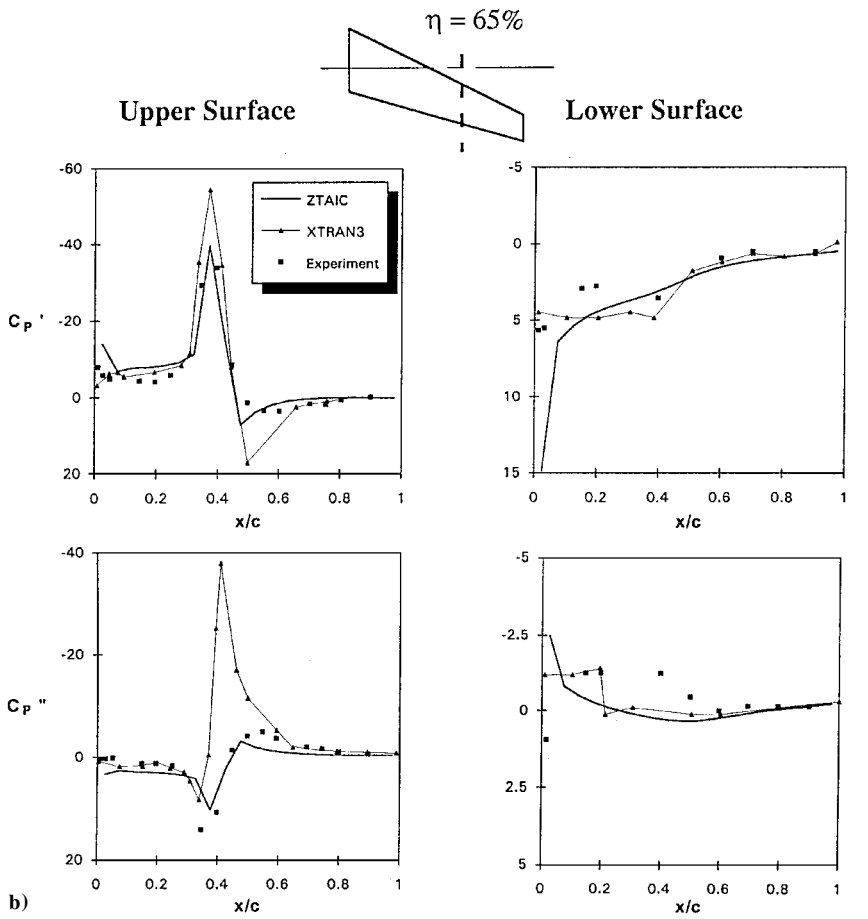

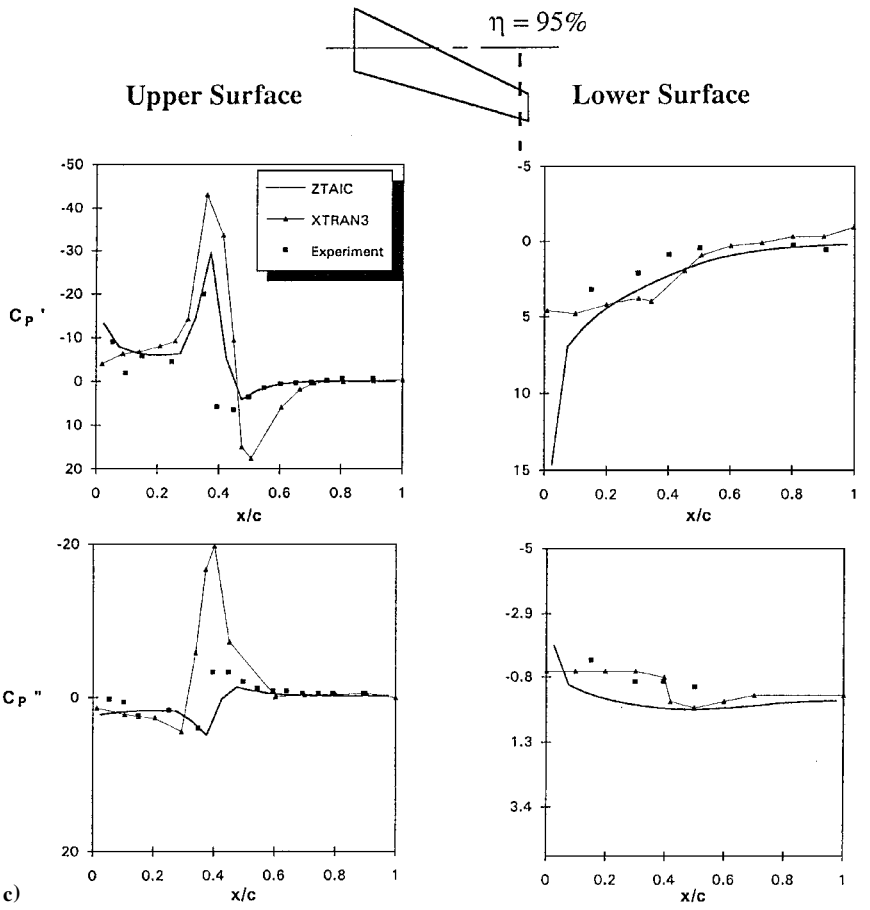

Fig. 4 LANN wing. In-phase and out-of-phase pressures in pitching oscillation about 62% root chord at three spanwise locations (M = 0.82 and k = 0.205) (continued).

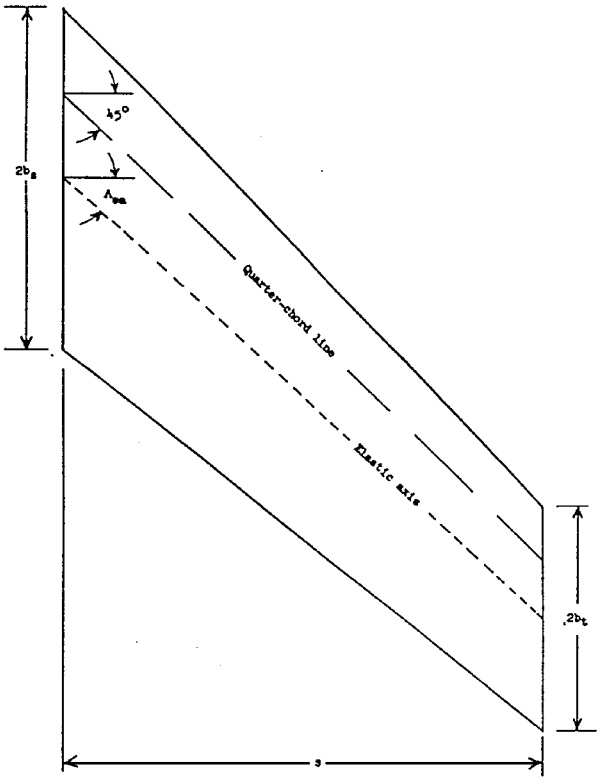

Fig. 5 AGARD standard 445.6 wing. Configuration shows the following dimensions: AR = 4.0, λ = 45 deg, Λ = 0.6, NACA 65A004 airfoil section (taken from AGARD Report 765 by Carson Yates).

the application of the modal-AIC procedure can be generalized. The baseline modes ϕ_{ij} in Eq. (5) can represent the vibration modes of a baseline structure, whereas h_{kj} are now the updated modes at a certain stage of a design cycle.

Transonic Equivalent Strip Method and Transonic AIC

To implement the preceding modal-based AIC approach, it is essential to select an unsteady transonic method that is computationally efficient. Among all existing methods that employ the transonic small disturbance equation (TSDE), the transonic equivalent strip (TES) method appears to be a viable candidate.[17] The simplicity of the TES input format and program structure allows a straightforward integration of the TES method with the modal AIC formulation.

The TES approach consists of two consecutive correction steps to a given nonlinear transonic small disturbance code such as ZTRAN,[17,18,19] namely, the chordwise mean flow correction and the spanwise phase correction. The computation procedure requires direct steady mean pressure input supplied by measured data or other CFD computation. It does not otherwise require the actual shape of each airfoil section or grid generation of a given planform. Therefore, except for the additional steady pressure input, the input data required by TES are very similar to that of a linear panel method such as DLM or ZONA6.[3]

Based on the same scheme formulated in Ref. 20, the TES approach can be recast into a new expression. Here, the transonic unsteady pressures can be expressed in terms of the linear unsteady pressures and a correction function fn, i.e.,

$$\Delta C^{N}_{P_3} = \Delta C^{\ell}_{P_3} + fn(\delta, \mu) \tag{8}$$

where $\delta = \delta(\Delta C^{N}_{P_2}, \Delta C^{\ell}_{P_3})$ is the chordwise-correction function and $\mu = \mu(\Delta C^{\ell}_{P3}, a\Delta C^{\ell}_{P_2})$ is the spanwise phase-correction function.

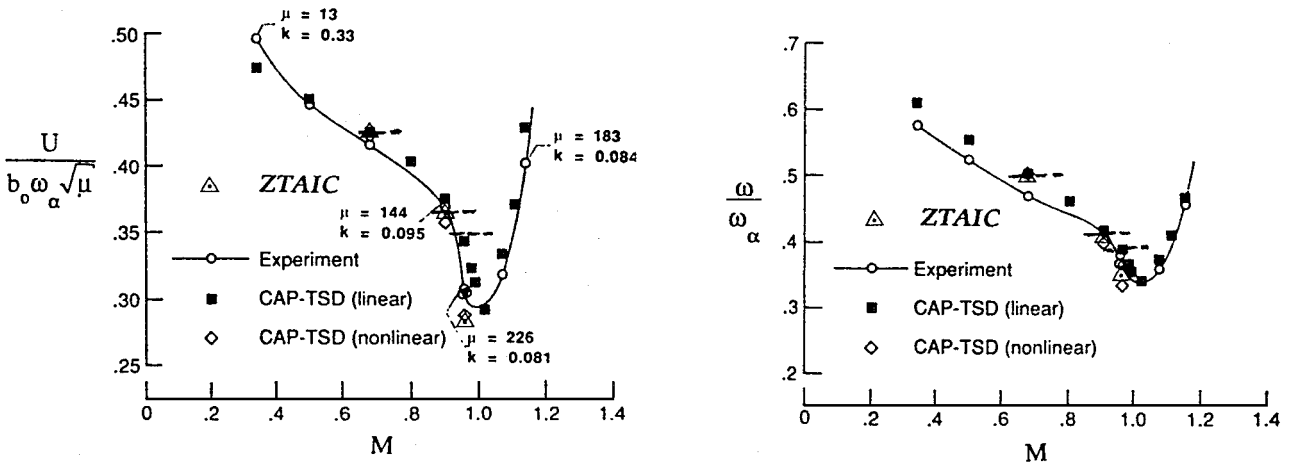

Fig. 6 Flutter speeds and flutter frequencies of 445.6 weakened wing (M = 0.678, 0.90, and 0.95).

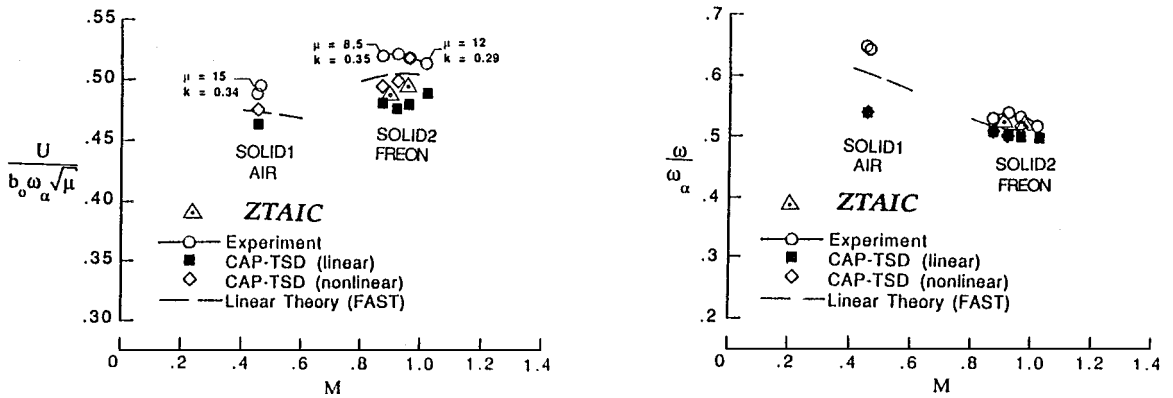

Fig. 7 Flutter speeds and flutter frequencies of 445.6 solid wing (M = 0.90 and 0.95).

Note that $\Delta C_{P_2}^{\ell}$ and $\Delta C_{P_3}^{\ell}$ are chordwise and three-dimensional linear unsteady pressures computed by DLM or ZONA6, where $\Delta C_{P_2}^{\mathcal{N}}$ is the transonic unsteady pressure as provided by the ZTRAN code. The chordwise correction function involves an inverse airfoil design procedure built into the ZTRAN, with which the local shock structure can be properly recovered according to the input pressure data. Clearly, the mean shock waves cannot be created or destroyed by this correction process. Thus, the modal AIC matrix of Eq. (7) can be generated by applying Eq. (8) to five basic modes, namely, the plunge, pitch, leading-edge flap, trailing-edge flap, and chordwise bending modes. Again, we note that the choice of a five basic-mode combination here is only a special practice of the general modal AIC formulations, Eqs. (4–6). For a typical wing structure such a choice should be sufficient to represent a given set of modes according to Eq. (6). The AIC method employs the combined procedure of modal AIC with the TES approach and is termed the TES/AIC or the TAIC method. Accordingly, a computer program called ZTAIC has been developed.

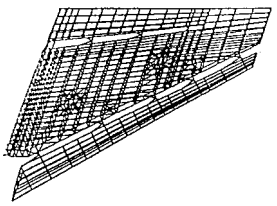

Fig. 8 Modeled F-16 wing. Structural model: AR = 2.8, 4% parabolic arc airfoil section.

Unsteady Pressures: Measured Data Input

Lessing Wing

Figure 1 shows the Lessing wing[21] with a rectangular planform of aspect ratio 3.0 and with a 5%-thick parabolic arc airfoil section. Unsteady pressure magnitudes and phase angles are presented in Figs. 2a and 2b for spanwise locations at $\eta = 0.5$, 0.7, and 0.9 ($\eta = 2y/b$). The ZTAIC results correlate reasonably well with two sets of experimental data (first and second runs).

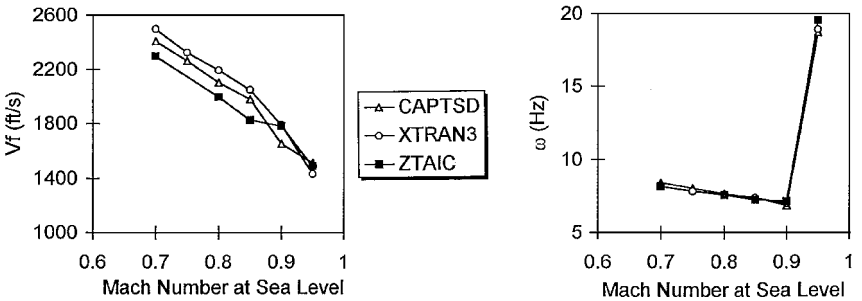

Fig. 9 Flutter speeds and frequencies of modeled F-16 wing computed by ZTAIC, CAPTSD, and XTRAN3S.

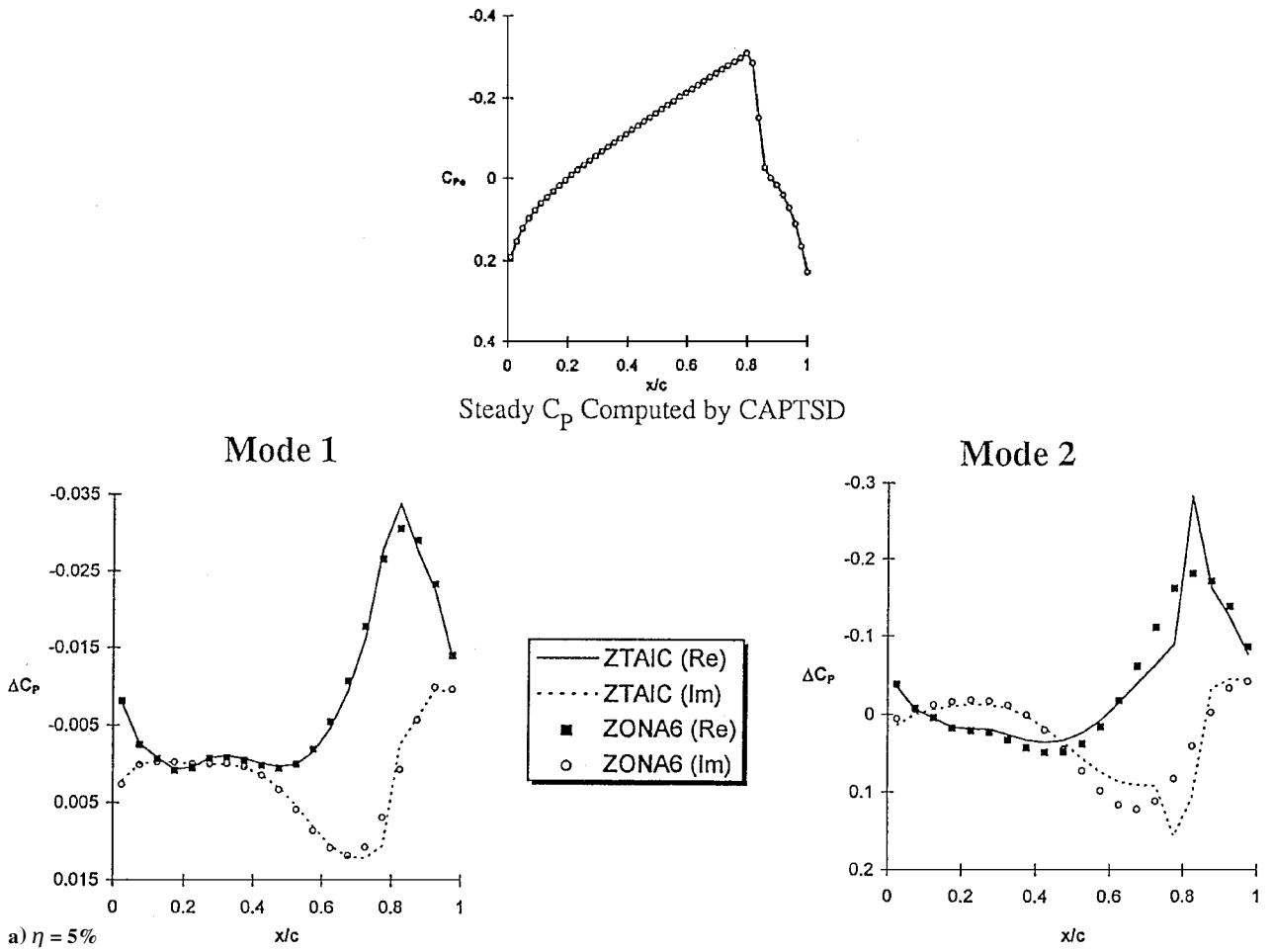

Fig. 10 Modeled F-16 wing. Unsteady pressures of the first bending and first torsion modes ($M = 0.925$ and $k = 1.0$).

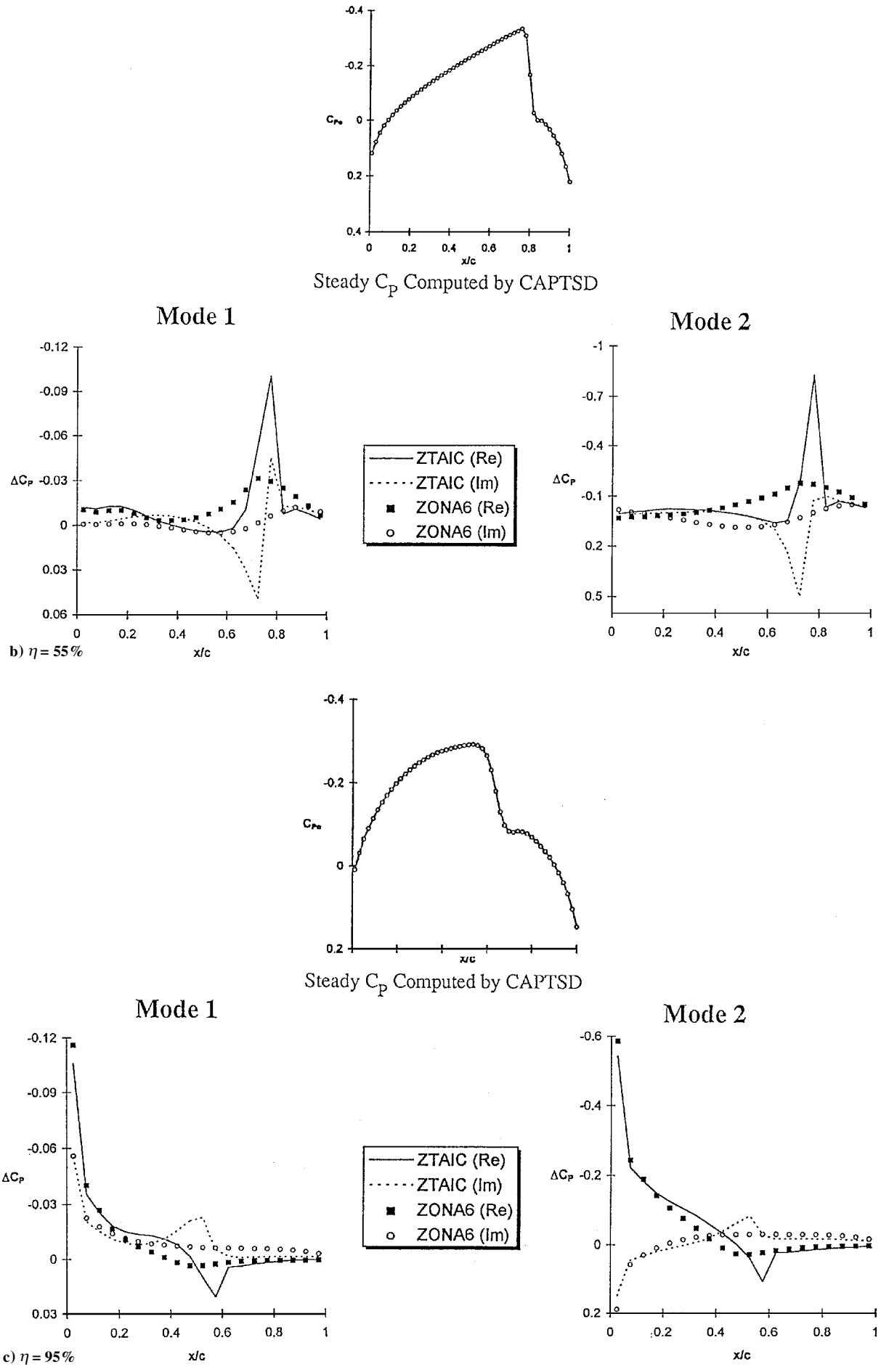

Fig. 10 Modeled F-16 wing. Unsteady pressures of the first bending and first torsion modes (M = 0.925 and k = 1.0) (continued).

Table 1 445.6 weakened wing flutter results

Test cases		Wind-tunnel data		ZONA6 – – – (linear)		ZTAIC △(nonlinear)		CAPTSD ◇ (nonlinear)	
M	ρ, slug/ft^3	ω_f, Hz	V_f, ft/s	ω_f, Hz	V_f, ft/s	ω_f, Hz	V_f, ft/s	ω_f, Hz	V_f, ft/s
0.678	0.000404	17.98	759.1	19.81	766.0	19.30	761.0	19.2	768
0.900	0.000193	16.09	973.4	16.31	984.0	16.38	965.2	15.8	952
0.950	0.000123	14.50	1008.4	16.18	1192.0	13.46	944.0	12.8	956

Table 2 445.6 solid wing flutter results

Test cases		Wind-tunnel data[a]		ZONA6 (linear)		ZTAIC[b] (nonlinear)		CAPTSD[a] (nonlinear)	
M	ρ, slug/ft^3	ω_f, Hz	V_f, ft/s	ω_f, Hz	V_f, ft/s	ω_f, Hz	V_f, ft/s	ω_f, Hz	V_f, ft/s
0.90	0.00357	27.00	452.0	26.75	439.0	25.71	418.0	25.8	435.0
0.95	0.00320	26.91	479.0	26.89	462.0	25.46	450.0	26.2	472.1

[a]Interpolated between Mach 0.87, 0.92, and 0.96. [b]Restart run using AICs of weakened wing (1 min CPU/case).

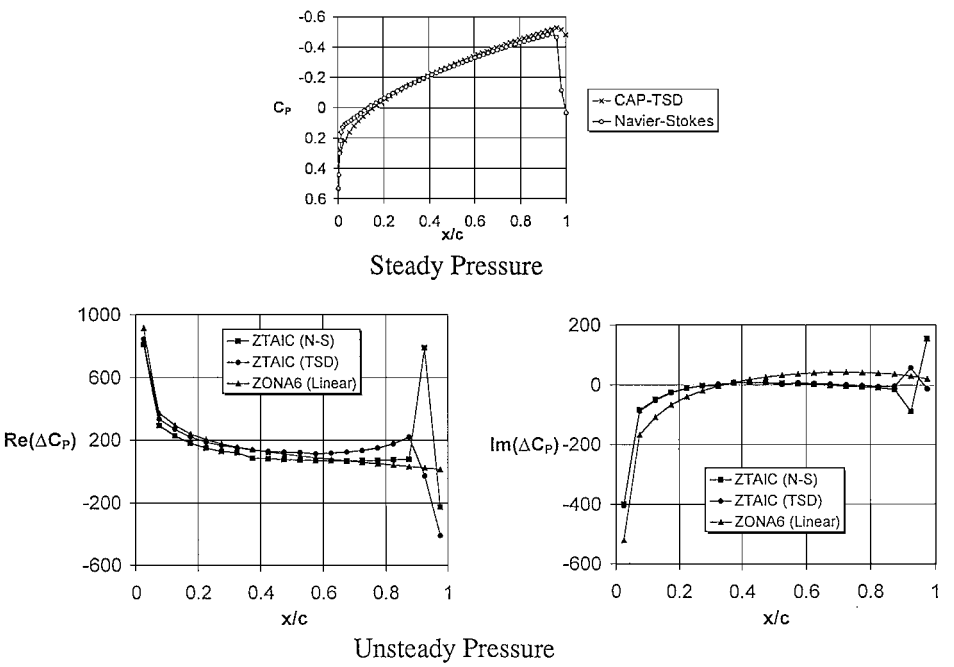

Fig. 11 Steady and unsteady pressure distribution for the Doggett wing with a 4%-thick parabolic arc section at M_∞ = 0.95, k = 0.14, and $2y/b$ = 0.45.

LANN Wing

Figure 3 shows the dimensions of the LANN wing[22–24] planform of aspect ratio 7.93 and a 12%-thick airfoil section. Figure 4 presents the in-phase and out-of-phase pressures of the LANN wing with pitching axis at 62% root chord. Throughout three spanwise locations considered ($\eta = 32.5$, 65, and 95%), the present results for the upper surface compare more favorably with NLR measured data than do the XTRAN3 results. Because subcritical flows are predicted for lower surfaces, the unsteady pressures do not contain the shock jump, as expected.

New Flutter Results: Computational Input

AGARD Standard 445.6 Wing

The 445.6 wing planform,[25] shown in Fig. 5, has an aspect ratio of 4 and a NACA 65A004 airfoil section. It has two structural models: the solid wing and the weakened wing. This is an ideal case to demonstrate ZTAIC's AIC capability. The aerodynamic shapes of these two models remain the same, but structurally they should have two different sets of baseline modes. However, these two sets of modes are subject to the same structural boundary conditions. For this reason the same modal AIC can be shared by both models. Hence, the modal AIC computed for the weakened wing can be saved allowing for a warm start for the solid wing. Figures 6 and 7 and Tables 1 and 2 present the flutter results of the weakened wing and solid wings, respectively. At a subsonic Mach number $M_\infty = 0.678$ the ZTAIC result is in good agreement with that of ZONA6, as expected. At other supercritical Mach numbers where $M_\infty = 0.9$ and 0.95, ZTAIC predicts a pronounced transonic dip that is comparable to that predicted by the CAP-TSD code.[20,26]

Modeled F-16 Wing

Figure 8 shows the structural model of the F-16 wing.[27] The wing planform has an aspect ratio of 2.8, with 4%-thick parabolic arc airfoil sections. Figure 9 presents the flutter speeds and frequencies at six Mach numbers: $M_\infty = 0.7$, 0.75, 0.8, 0.85, 0.9, and 0.95. The flutter results of ZTAIC are in good agreement with those of XTRAN3S and CAP-TSD, especially at $M_\infty = 0.95$. Notice that the flutter (modal) mechanism changes from $M_\infty = 0.9$ to 0.95, as indicated by the jump in the flutter frequency (from 6.8 to 19 Hz). ZTAIC concurs with the other two codes in the prediction of this mechanism. Steady and unsteady pressures at $M_\infty = 0.925$ are presented in Figs. 10a–10c at three spanwise locations ($\eta = 5$, 55, and 95%).

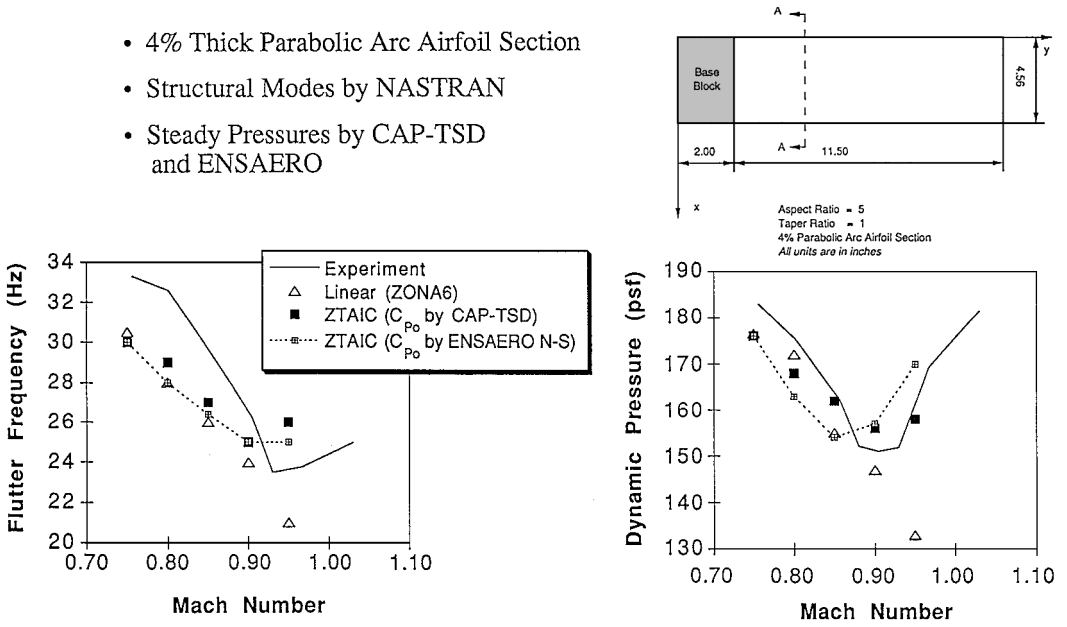

Fig. 12 Flutter dynamic pressures and frequencies of the Doggett wing at five mach numbers: M_∞ = 0.75, 0.8, 0.85, 0.9, and 0.95.

While the steady pressure input data are computed by CAP-TSD,[26] the unsteady pressures are presented for two modes (mode 1 being the first bending and mode 2 the first torsion) at a reduced frequency $k = 1.0$. Unlike the 445.6 wing aerodynamics, strong shocks are present at the first two inboard span stations. The shock strength is somewhat weakened at the tip, where, as expected, the ZTAIC results approach those of ZONA6, except at the shock and its vicinity.

Doggett Wing

The Doggett wing[28] under investigation is a rectangular planform with aspect ratio of 5.0 and a 4%-thick parabolic arc airfoil section. The structural modes of the Doggett wing are obtained from the NASTRAN/FEM modeling. The steady pressure inputs used are the computed pressures by CAP-TSD[9] and ENSAERO,[26] whereas the unsteady pressures are computed by ZTAIC.

Figure 11 presents the steady and unsteady pressure distributions of the Doggett wing at $M_\infty = 0.95, k = 0.14$, and at a 45% semispanwise location. ENSAERO predicts a shock location slightly ahead of the one predicted by CAP-TSD near the airfoil trailing edge. The viscous effect (introduced by the N-S option of ENSAERO) and hence the transonic shock behavior has much to do with changes in the flutter boundary of the wing (see Fig. 12).

Figure 12 presents the flutter dynamic pressures and flutter frequencies at five Mach numbers: $M_\infty = 0.75, 0.8, 0.85, 0.9$, and 0.95. ZTAIC using both pressure inputs predicts similar flutter trends to that of the measured data. Linear theory (ZONA6), by contrast, predicts a conservative but meaningless flutter trend at higher transonic Mach numbers. At a subsonic Mach number, $M_\infty = 0.75$, the flutter point predicted by ZONA6 is found to depart largely from the measured data.

Conclusions

A TAIC method has been developed as an efficient tool for flutter, aeroservoelastic, and MDO applications. The generated computer code ZTAIC has been validated with measured and computed results in unsteady pressures and flutter analysis for various wing planforms. In contrast to the current transonic CFD practice, ZTAIC appears to have the following salient features:

1) Grid generation is not required.

2) It is essentially a unified transonic/subsonic lifting surface method in that the input format is the same as that of DLM except the additional pressure input. The thickness effect in the unsteady flow is introduced by an inverse design procedure according to the given pressure input. When the pressure input is removed, the method reduces to a subsonic lifting surface method (ZONA6).

3) The steady pressure input is an option (in the program) that can be supplied by measured data or by CFD computation. In this way the proper unsteady shock location and strength can be ensured.

4) The advantage of the built-in AIC capability in ZTAIC is threefold. First, it allows ZTAIC to perform a rapid aeroelastic analysis where the saved AIC can be easily retrieved for repeated applications. This procedure is most desirable in the preliminary design stage where the aerodynamic configuration has been determined. Second, the modal-AIC formulation renders ZTAIC readily integrable with the structural FEM in an MDO environment such as ASTROS. Third, the s-domain aerodynamics necessary for aeroservoelasticity can be easily generated from the k-domain solution yielded by the AIC approach.

Acknowledgments

The authors thank A. G. Striz and S. Y. Jung of the University of Oklahoma for providing steady pressure solutions from the ENSAERO computation of the Doggett wing. The authors thank Ray Kolonay of Wright Laboratory for providing the CAP-TSD flutter results and the structural information of the 445.6 wing and the modeled F-16 wing. The provision of the CAP-TSD code by Tom Noll of NASA Langley and David Schuster of Lockheed-Martin is gratefully acknowledged.

References

[1]Rodden, W. P., Giesing, J. P., and Kalman, T. P., "New Developments and Applications of the Subsonic Doublet Lattice Methods for Non-Planar Configurations," AGARD CP-80-71, Pt. 2, No. 4, 1971.

[2]Chen, P. C., and Liu, D. D., "A Harmonic Gradient Method for Unsteady Supersonic Flow Calculations," *Journal of Aircraft*, Vol. 22, No. 5, 1985, pp. 371–379.

[3]Chen, P. C., and Liu, D. D., "Unsteady Supersonic Computations of Arbitrary Wing-Body Configurations Including External Stores," *Journal of Aircraft*, Vol. 27, No. 2, 1990, pp. 108–116.

[4]Chen, P. C., Lee, H. W., and Liu, D. D., "Unsteady Subsonic Aerodynamics for Bodies and Wings with External Stores Including Wake Effect," International Forum on Aeroelasticity and Structural Dynamics, Paper 91-060, June 1991; also, *Journal of Aircraft*, Vol. 30, No. 5, 1993, pp. 618–628.

[5]Hounjet, M. H. L., "Calculation of Unsteady Subsonic and Supersonic Flow About Oscillating Wings and Bodies by New Panel Methods," National Aerospace Lab., TP89119U, April 1989.

[6]Karpel, M., "Design for Active and Passive Flutter Suppression and Gust Alleviation," NASA CR-3482, 1981.

[7]Abel, I., Newsom, J. R., and Dunn, H. J., "Application of Two Synthesis Methods for Active Flutter Suppression on an Aeroelastic Wing-Tunnel

Model," *Proceedings of the AIAA Atmospheric Flight Mechanics Conference for Future Space Systems*, AIAA, New York, 1979, pp. 93–107.

[8]Edwards, J. W., and Malone, J. B., "Current Status of Computational Methods for Transonic Unsteady Aerodynamics and Aeroelastic applications," AGARD Structures and Material Panel Specialists Meeting on Transonic Unsteady Aerodynamics and Aeroelasticity, Paper 1, Oct. 1991.

[9]Guruswamy, G. P., "ENSAERO—A Multidisciplinary Program for Fluid/Structural Interaction Studies of Aerospace Vehicles," *Computing System Engineering*, Vol. 1, Nos. 2–4, 1990, pp. 237–256.

[10]Johnson, E. H., and Venkayya, V. B., "Automated Structural Optimization System (ASTROS), Theoretical Manual," Air Force Wright Aeronautical Lab., AFWAL-TR-88-3028, Vol. 1, Dec. 1988.

[11]Neill, D. J., and Herendeen, D. L., "ASTROS Enhancements, Volume I/II/III—ASTROS User's Manual/Programmer's Manual/Theoretical Manual," Air Force Wright Aeronautical Lab., WL-TR-96-3004/3005/3006, May 1995.

[12]Kapania, R., Bhardwaj, M., Reichenbach, E., and Guruswamy, G., "Aeroelastic Analysis of Modern Complex Wings," AIAA Paper 96-4011, Sept. 1996.

[13]Chen, P. C., Liu, D. D., Sarhaddi, D., Striz, F., Neill, D., and Karpel, M., "Enhancement of the Aeroservoelastic Capability in ASTROS," WL-TR-96-3119, Wright–Patterson AFB, Ohio, May 1996.

[14]Liu, D. D., Yao, Z. X., Sarhaddi, D., and Chavez, F., "Piston Theory Revisited and Further Applications," International Council of the Aeronautical Sciences, ICAS Paper 94-2.8.4, Sept. 1994.

[15]Liu, D. D., Chen, P. C., Yao, Z. X., and Sarhaddi, D., "Recent Advances in Lifting Surface Methods," *The Aeronautical Journal of the Royal Aeronautical Society*, Vol. 100, No. 958, 1996, pp. 327–339.

[16]Dowell, E. H., Bland, S. R., and Williams, M. H., "Linear/Nonlinear Behavior in Unsteady Transonic Aerodynamics," *AIAA Journal*, Vol. 21, No. 1, 1983.

[17]Liu, D. D., Kao, Y. F., and Fung, K. Y., "An Efficient Method for Computing Unsteady Transonic Aerodynamics of Swept Wings with Control Surfaces," *Journal of Aircraft*, Vol. 25, No. 1, 1988, pp. 25–31.

[18]"ZTES/TAIC Documentation," ZONA Technology, Inc., Rept. 93-06, Scottsdale, AZ, Sept. 1993.

[19]Ballhaus, W. F., and Goorjian, P. M., "Implicit Finite-Difference Computations of Unsteady Transonic Flows About Airfoils," *AIAA Journal*, Vol. 15, No. 12, 1977, pp. 1728–1735.

[20]Batina, J. T., "An Efficient Algorithm for Solution of the Unsteady Transonic Small-Disturbance Equation," *Journal of Aircraft*, Vol. 25, No. 7, 1988, pp. 598–605.

[21]Lessing, H. C., Troutman, J. L., and Menees, G. P., "Experimental Determination of the Pressure Distribution on a Rectangular Wing Oscillating in the First Bending Mode for Mach Numbers from 0.24 to 1.30," NASA TN D-33, Dec. 1960.

[22]Malone, J. B., and Ruo, S. Y., "LANN Wing Test Program: Acquisition and Application of Unsteady Transonic Data for Evaluation of Three-Dimensional Computational Methods," Air Force Wright Aeronautical Lab., AFWAL-TR-83-3006, Feb. 1983.

[23]Sotomayer, W. A., and Borland, C. J., "Numerical Computation of Unsteady Transonic Flow About Wings and Flaps," AIAA Paper 85-1712, 1985.

[24]Horsten, J. J., Den Boer, R. G., and Zwaan, R. J., "Unsteady Transonic Pressure Measurements on a Semi-Span Wing Tunnel Model of a Transport-Type Supercritical Wing (LANN Model)," NLR TR-82-069U, Pts. 1 and 2, and AFWAL-TR-83-3039, Pts. 1 and 2, Wright–Patterson AFB, Ohio, March 1993.

[25]Yates, E. C., Jr., "AGARD Standard Aeroelastic Configurations for Dynamic Response I-Wing 445.6," AGARD-R 765, July 1988.

[26]Bennett, R. M., Batina, J. T., and Cunningham, H. J., "Wing-Flutter Calculations with the CAP-TSD Unsteady Transonic Small-Disturbance Program," *Journal of Aircraft*, Vol. 26, No. 9, 1989, pp. 876–882.

[27]Kalonay, R., "Unsteady Aeroelastic Optimization in the Transonic Regime," AIAA Paper 96-3983, Sept. 1996.

[28]Doggett, R. V., Jr., Rainy, A. G., and Morgan, H. G., "An Experimental Investigation of Aerodynamic Effects of Airfoil Thickness on Transonic Flutter Characteristics," NASA TM X-79, Nov. 1959.